

Exact Minimum Control Switch Motion Planning for the Snakeboard

Stefano Iannitti Kevin M. Lynch

Mechanical Engineering Dept.

Northwestern University

Evanston, IL 60208 USA

stefano.iannitti@asi.it

kmlynch@northwestern.edu

Abstract— We study the problem of computing an exact motion plan for the snakeboard by exploiting its kinematic controllability properties and its *decoupling vector fields*. Decoupling vector fields allow us to treat the underactuated dynamic system as a kinematic one, and rest-to-rest paths are the concatenation of integral curves of the decoupling vector fields. These paths can then be time-scaled according to actuator limits to yield fast trajectories. Switches between decoupling vector fields must occur at zero velocity, so to find fast trajectories, we wish to find paths minimizing the number of switches. In this paper we solve the minimum switch path planning problem for the snakeboard. We consider two problems: (1) finding motion plans achieving a desired position and orientation of the body of the snakeboard, and (2) the full problem of motion planning for all five configuration variables of the snakeboard. The first problem is solvable in closed form by geometric considerations, while the second problem is solved by a numerical approach with guaranteed convergence. We present a complete characterization of the snakeboard’s optimal paths in terms of the number of switches.

I. INTRODUCTION

The snakeboard is a commercial toy whose concept is derived from the well known skateboard. It is composed of two steerable wheeled platforms joined by a coupling bar, and the rider propels himself forward without touching the ground by steering the wheels and twisting his body back and forth. A simple model of the snakeboard is shown in Figure 1. Here a momentum rotor simulates the rider by spinning, and by conservation of angular momentum about the rotation center chosen by the wheels, the snakeboard body moves. The snakeboard model is an underactuated mechanical system with nonholonomic constraints. It is underactuated because it has only two control torques, to spin the wheels and the rotor, while the configuration space is five-dimensional. The nonholonomic constraints express the fact that the wheels roll without slip, and without these constraints, the snakeboard would be unable to locomote.

The dynamics of the simplified snakeboard model with two inputs and five configuration variables were first studied in [15], where periodic controls were shown to generate various gaits. The first proof of local controllability of the snakeboard was given by Ostrowski and Burdick [16], exploiting properties of systems with symmetry and constraints. Ostrowski [18] derived an approximate motion planning algorithm for the snakeboard, extending the approach of steering using periodic inputs described by Murray and Sastry [14] for kinematic systems. A nu-

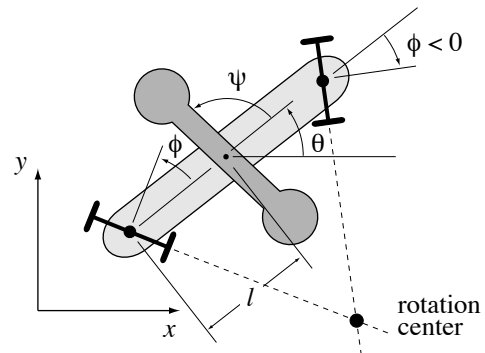


Fig. 1. The snakeboard model.

merical method for optimal trajectory generation has also been described by Ostrowski, Desai, and Kumar [19]. Recently, an analytical solution for the motion planning problem was given by Bullo and Lewis [3], exploiting the notion of *kinematic controllability* introduced in [13], [5] and extended to mechanical systems with constraints [4]. (See also [11], [6], [12] for more background on constrained mechanical systems.)

While ideally we might like to find energy- or time-optimal motions for the snakeboard, an approximate solution to such a problem requires solving a computationally complex nonlinear program [19]. It is also difficult to incorporate obstacle constraints. For this reason, we pursue an approach to sub-time-optimal trajectory planning based on *decoupling* the problem into kinematic path planning followed by time scaling of the path to produce a trajectory. Exact kinematic paths can be found in closed-form in the absence of obstacles, and in the presence of obstacles, the computational complexity of the search for a plan is greatly reduced by restricting the search to the configuration space instead of the full state space. Time-scaling a motion along a path subject to actuator limits can be done in a computationally efficient manner (see, for example, [2], [21] for algorithms finding the time-optimal trajectory of a *fully actuated* system along a path). This decoupled approach offers the possibility of real-time trajectory planning in environments with obstacles. A first example of this decoupled approach for underactuated systems can be found in (Lynch *et al.* [13]), where it is applied to a three DOF manipulator with the third joint passive.

This decoupled approach to trajectory planning is possible due to the kinematic controllability of the snakeboard. Kinematic controllability implies that the snakeboard possesses a set of *decoupling vector fields* — velocity vector fields whose integral curves can be followed at any speed and acceleration. Kinematic path planning is achieved by concatenating segments

of these integral curves. Switches between decoupling vector fields must occur at zero velocity (otherwise the velocity would be discontinuous), so we are interested in minimizing the number of switches in the path planning phase. This paper solves the problem of planning a path for the snakeboard minimizing the number of switches between decoupling vector fields. Although the notion of kinematic controllability has been exploited by Bullo and Lewis [3] to perform motion planning, no attention was given to minimizing the number of switches between decoupling vector fields.

Because we can treat the dynamic underactuated system as a kinematic one, our motion planning problem is reminiscent of motion planning for a kinematic car. The problem of finding shortest paths in the plane for a kinematic car with a minimum turning radius was studied by Dubins [8] for a forward-only car and Reeds and Shepp [20] for a car that can reverse. The results of Reeds and Shepp have been sharpened and extended by Sussmann and Tang [23] and Souères and Laumond [22]. In related work, Balkcom and Mason [1] derived the minimum-time motions for a kinematic differential drive car subject to wheel velocity limits.

While the car-like robot systems described above can be treated naturally as driftless kinematic systems (Lewis [10]), the *kinematic reduction* of a dynamic underactuated system such as the snakeboard is not as straightforward. In Section II we review the concepts of decoupling vector fields and kinematic reductions, and in Section III we give the snakeboard model and describe the decoupling vector fields. Section IV formalizes two different path planning problems: (1) achieving a desired position and orientation for the snakeboard body only (Section V), and (2) achieving a desired configuration for all five configuration variables (Section VI). In each section, we give the minimum number of distinct integral curve segments required to accomplish the task, as a function of the initial and goal configuration, as well as example sequences of vector fields solving the problem. These sequences are reminiscent of the Reeds-Shepp curves for kinematic cars, except that Reeds-Shepp curves use only straight line motions and minimum turning radius motions to achieve shortest paths, whereas we use the ability to control the turning radius to minimize the number of distinct motion segments. The motion plans are completed by finding the time each vector field must be followed. The complete plan can be found in closed form for the first planning problem, while the second problem is solved by a numerical approach with guaranteed convergence.

II. REVIEW OF KINEMATIC REDUCTIONS

Here we review ideas that allow us to treat the snakeboard as a kinematic system, adapted from [13], [5], [4].

A second-order underactuated dynamic system subject to nonholonomic velocity constraints can be written in the form

$$\begin{aligned} M(q)\ddot{q} + C(q, \dot{q})\dot{q} &= T(q)u + A^T(q)\lambda \\ A(q)\dot{q} &= 0, \end{aligned} \quad (1)$$

where $q \in \mathcal{Q} = \mathbb{R}^n$ is a vector of generalized coordinates; $u \in \mathbb{R}^m$ is a vector of generalized control forces, where $m < n$; $M(q)$ is a full-rank $n \times n$ inertia matrix; $C(q, \dot{q})\dot{q} \in \mathbb{R}^n$ is a

vector of centrifugal and Coriolis terms with C linear in \dot{q} ; $T(q)$ is an $n \times m$ matrix indicating how the control forces u act on the generalized coordinates; $A(q)$ is a $k \times n$ matrix describing the k Pfaffian velocity constraints $A(q)\dot{q} = 0$; and $A^T(q)\lambda$ is a set of constraint forces, where $\lambda \in \mathbb{R}^k$ are Lagrange multipliers. Since the constraints (2) are satisfied throughout the motion, they can be differentiated to give

$$A(q)\ddot{q} + \dot{A}(q)\dot{q} = 0. \quad (3)$$

Solving (1) for \ddot{q} , substituting into (3), solving for λ and plugging back into (1), we can eliminate the Lagrange multipliers, getting the form

$$P(q)(\ddot{q} + M^{-1}(q)C(q, \dot{q})\dot{q}) = P(q)M^{-1}(q)T(q)u, \quad (4)$$

where

$$P(q) = I - M^{-1}(q)A^T(q)(A(q)M^{-1}(q)A^T(q))^{-1}A(q)$$

and I is the identity matrix. (See, for example, [12].) The $n \times n$ matrix $P(q)$ is rank $n - k$ and projects general motions to the $n - k$ directions satisfying the constraints. Thus (4) and (2) specify n linearly independent equations for the system's n degrees-of-freedom.

Consider a motion of the system $q(t)$ satisfying the velocity constraints (2) such that there exists a control u satisfying (4) for any arbitrary time-scaling of the motion $q(s(t))$, $s(t) \in \mathbb{R}$ and twice-differentiable. Then $q(t)$ is said to be a *kinematic* motion for the system. If the integral curves of a velocity vector field $X(q)$ are kinematic motions, then $X(q)$ is called a *decoupling vector field*. We call the first-order kinematic control system

$$\dot{q} = X(q)w(t), \quad w(t) \in \mathbb{R} \text{ and continuous}$$

a (rank one) *kinematic reduction* of the dynamic system, meaning that any trajectory of the kinematic reduction can be realized by the full dynamic system. This means that if we restrict the possible motions of the full dynamic system to motion along decoupling vector fields, we can treat the system as if it were a kinematic system. We say that the system is *locally kinematically controllable* at q if there exists a set of decoupling vector fields $\{X_1(q), \dots, X_p(q)\}$ such that the Lie algebra of these vector fields spans the tangent space $T_q\mathcal{Q}$. If the system is locally kinematically controllable at all q , then it is *kinematically controllable* and any equilibrium configuration on \mathcal{Q} is reachable by flowing along the decoupling vector fields.

The conditions for a decoupling vector field can be equivalently interpreted geometrically. Defining the *affine connection* ∇ associated with the kinetic energy metric $M(q)$ on the configuration space \mathcal{Q} , the *covariant derivative* of a vector field $Y_2(q)$ with respect to $Y_1(q)$ can be written

$$\nabla_{Y_1(q)}Y_2(q) = \frac{\partial Y_2(q)}{\partial q}Y_1(q) + Y_1^T(q)\Gamma(q)Y_2(q),$$

where $\Gamma(q)$ is the $n \times n \times n$ matrix of *Christoffel symbols* associated with $M(q)$, and $Y_1^T\Gamma Y_2$ is appropriately defined.¹ Then the unconstrained dynamics of the system can be written

$$\nabla_{\dot{q}}\dot{q} = \ddot{q} + \dot{q}^T\Gamma(q)\dot{q} = \ddot{q} + M^{-1}(q)C(q, \dot{q})\dot{q} = M^{-1}(q)T(q)u,$$

¹A common alternative definition of the Christoffel symbols is Γ' , where $Y_1^T\Gamma Y_2 = M^{-1}Y_1^T\Gamma'Y_2$.

and the constrained dynamics (4) can be written

$$P(q)\nabla_{\dot{q}}\dot{q} = P(q)M^{-1}(q)T(q)u.$$

We call the m columns of $P(q)M^{-1}(q)T(q)$ the *input vector fields* $Y_i(q)$, $i = 1 \dots m$, and the collection of these vector fields is written $\mathcal{Y} = \{Y_1, \dots, Y_m\}$. Then a vector field $X(q)$ is a decoupling vector field if and only if $X \in \text{span}(\mathcal{Y})$ and $P\nabla_X X \in \text{span}(\mathcal{Y})$.

With a collection of decoupling vector fields, motion planning between zero-velocity states becomes the problem of finding a concatenation of segments of integral curves of these vector fields leading from the initial to the goal configuration. Switches between the decoupling vector fields must occur at zero velocity, so for fast path execution, it is useful to find motions minimizing the number of switches needed between vector fields. It is precisely this problem that this paper solves for the snakeboard.

III. THE SNAKEBOARD MODEL

A dynamic model of the snakeboard in Figure 1 can be found in the seminal work [15]; we will use a model similar to that in [3], and review the development of the equations of motion. The snakeboard has a five-dimensional configuration space described by the coordinate vector $q = (x, y, \theta, \psi, \phi) \in \mathcal{Q} = SE(2) \times \mathbb{S} \times [-\frac{\pi}{2}, \frac{\pi}{2}]$, as shown in Fig. 1. Specifically, (x, y) represents the cartesian position of the center of the snakeboard coupler, θ is its angle, and ψ and ϕ are the angle of the rotor and the steering angle of the wheels, respectively, expressed in the body frame. (We point out that our definition of ϕ is the negative of that used in [3].)

The matrices $M(q)$ and $T(q)$ are

$$M = \begin{bmatrix} m & 0 & 0 & 0 & 0 \\ 0 & m & 0 & 0 & 0 \\ 0 & 0 & J + J_r + J_w & J_r & 0 \\ 0 & 0 & J_r & J_r & 0 \\ 0 & 0 & 0 & 0 & J_w \end{bmatrix}, \quad T = \begin{bmatrix} 0 & 0 \\ 0 & 0 \\ 0 & 0 \\ 1 & 0 \\ 0 & 1 \end{bmatrix},$$

where m is the total mass of the snakeboard, J is the inertia of the coupler about its center of mass, J_r is the rotor inertia, $\frac{1}{2}J_w$ is the inertia of each set of wheels about its pivot point, and $u = (u_\psi, u_\phi)^T$ are the control torques at the rotor and the steering wheels. The wheels are assumed to roll without lateral slipping, defining the constraint matrix

$$A(q) = \begin{bmatrix} \sin \phi & 0 & -\ell \cos \theta \cos \phi & 0 & 0 \\ 0 & \sin \phi & -\ell \sin \theta \cos \phi & 0 & 0 \end{bmatrix}.$$

We define the input vector fields Y_ψ, Y_ϕ to be the columns of $P(q)M^{-1}(q)T(q)$, where $P(q)$ is determined by $M(q)$ and $A(q)$ as described in the previous section:

$$Y_\psi = \frac{c_1(\phi)}{J_r c_2(\phi)} \left(a(\phi) \left(\cos \theta \frac{\partial}{\partial x} + \sin \theta \frac{\partial}{\partial y} \right) - b(\phi) \frac{\partial}{\partial \theta} + \frac{\partial}{\partial \psi} \right)$$

$$Y_\phi = \frac{1}{J_w} \frac{\partial}{\partial \phi}$$

where

$$a(\phi) = -J_r \ell \cos(\phi) \sin(\phi) / c_1(\phi)$$

$$b(\phi) = J_r \sin^2(\phi) / c_1(\phi)$$

$$c_1(\phi) = m \ell^2 \cos^2(\phi) + (J + J_r + J_w) \sin^2(\phi)$$

$$c_2(\phi) = m \ell^2 \cos^2(\phi) + (J + J_w) \sin^2(\phi).$$

The equations of motion are

$$P(q)\nabla_{\dot{q}}\dot{q} = Y_\psi(q)u_\psi + Y_\phi(q)u_\phi.$$

The vector fields Y_ϕ , rotating the steering wheels, and Y_ψ , motion of the snakeboard by conservation of angular momentum as the rotor spins, are themselves decoupling. For convenience, we will choose scaled versions as our decoupling vector fields,

$$X_1 = J_w Y_\phi, \quad X_2 = \frac{J_r c_2(\phi)}{c_1(\phi)} Y_\psi.$$

Bullo and Lewis [3] showed that the system is kinematically controllable by these two decoupling vector fields.

Because the coefficients of $\frac{\partial}{\partial \phi}$ in X_1 and $\frac{\partial}{\partial \psi}$ in X_2 are unit, the (signed) travel time along X_1 and X_2 are equivalent to the change in the steering wheel angle $\Delta\phi$ and the change in the rotor angle $\Delta\psi$, respectively. Following X_1 for a time $\Delta\phi$ leads from an initial configuration q_0 to a final configuration $q_f = (x_0, y_0, \theta_0, \psi_0, \phi_0 + \Delta\phi)$, while following X_2 for a time $\Delta\psi$ from an initial configuration $q_0 = (0, 0, 0, 0, \phi_0)$ leads to a final configuration $(x, y, \theta, \Delta\psi, \phi_0)$, where

$$(x, y, \theta) = (\ell \cot \phi_0 \sin(-b(\phi_0)\Delta\psi), \ell \cot \phi_0 (1 - \cos(-b(\phi_0)\Delta\psi)), -b(\phi_0)\Delta\psi). \quad (5)$$

Note that when $\phi_0 = 0$, no actuation of the rotor produces motion of the coupler. We allow $\phi = \pm\pi/2$, so that the snakeboard can spin in place. This is possible by outfitting the snakeboard with “training wheels” to prevent it from falling over. We have built such a snakeboard in our lab.

The snakeboard dynamics are invariant to the configuration variables x, y, θ, ψ but not invariant to the wheel angle ϕ . This allows us to consider only motions starting from $q_0 = (0, 0, 0, 0, \phi_0)$ without loss of generality.

IV. PATH PLANNING FOR THE SNAKEBOARD

We consider the problem of steering the snakeboard from the initial configuration $q_0 = (0, 0, 0, 0, \phi_0)$ to the goal configuration $q_G = (x_G, y_G, \theta_G, \psi_G, \phi_G)$ using the decoupling vector fields X_1 and X_2 .

To keep the notation compact, we denote a motion of the steering wheels (along the vector field X_1) by the letter \mathcal{W} , and a motion due to the spinning of the rotor (along the vector field X_2) by the letter \mathcal{R} . Therefore, a plan \mathcal{P} consisting of steering the wheels followed by spinning the rotor is denoted by $\mathcal{P} = \mathcal{W}\mathcal{R}$.

To completely specify a plan, we add subscripts to the letters:

- \mathcal{W}_ϕ denotes a motion that steers the wheels to an angle ϕ ,
 - \mathcal{R}_ψ denotes a motion due to driving the rotor angle to ψ .
- Usually it is more convenient to denote the action of the rotor by its change in angle $\Delta\psi$. In this case, the action will be denoted by $\mathcal{R}_{\Delta\psi}$.

A plan \mathcal{P} is composed of a sequence of symbols \mathcal{R} and \mathcal{W} and their subscripts. Note, however, that

$$\mathcal{W}_{\phi_1} \mathcal{W}_{\phi_2} = \mathcal{W}_{\phi_2},$$

$$\mathcal{R}_{\Delta\psi_1} \mathcal{R}_{\Delta\psi_2} = \mathcal{R}_{\Delta\psi_1 + \Delta\psi_2},$$

so that an optimal plan \mathcal{P} never contains consecutive \mathcal{W} or \mathcal{R} symbols.

We define the length of a plan \mathcal{P} to be $l(\mathcal{P})$, the total number of motions \mathcal{W} and \mathcal{R} in the plan. Given an initial configuration q_0 and a final configuration q_G , we define $l_{\min}(q_0, q_G)$ to be the length of the shortest plan connecting q_0 to q_G . If the goal is expressed as a set of configurations \mathcal{Q}_G rather than a single configuration q_G , then $l_{\min}(q_0, \mathcal{Q}_G)$ denotes the length of the shortest plan to any point in \mathcal{Q}_G . In particular, the goal may be to simply transfer the body of the snakeboard to a desired configuration in $SE(2)$, ignoring the wheel and rotor angles.

The reduced problem (RP). Given an initial configuration of the snakeboard $q_0 = (x_0, y_0, \theta_0, \psi_0, \phi_0) = (0, 0, 0, 0, \phi_0)$ and a two-dimensional goal configuration manifold $\mathcal{Q}_1 = \{q | q = (x_G, y_G, \theta_G, \cdot, \cdot)\}$, compute a plan \mathcal{P} connecting q_0 to \mathcal{Q}_1 such that $l(\mathcal{P}) = l_{\min}(q_0, \mathcal{Q}_1)$.

Since three coordinates are being steered to their final values, generically three motions \mathcal{W} and \mathcal{R} are required.² (In this context, a generic problem is one where the initial and final configurations do not lie in particular lower-dimensional submanifolds of the configuration space.) Some problems may require more motions, but never more than six, as will be shown shortly.

The full problem can be stated as follows.

The full problem (FP). Given an initial configuration of the snakeboard $q_0 = (x_0, y_0, \theta_0, \psi_0, \phi_0) = (0, 0, 0, 0, \phi_0)$ and a desired configuration $q_G = (x_G, y_G, \theta_G, \psi_G, \phi_G)$, compute a plan \mathcal{P} connecting q_0 to q_G such that $l(\mathcal{P}) = l_{\min}(q_0, q_G)$.

All five coordinates need to be set to their final values, meaning that for a generic problem, five motions \mathcal{W} and \mathcal{R} are required. Some initial and final configurations may require more motion segments, but never more than seven.

In the next two sections we solve the problems RP and FP.

V. THE REDUCED PROBLEM

Problem RP, finding a motion sequence to move the coupler of the snakeboard from one configuration in $SE(2)$ to another, is a geometric problem. Since we will be focusing only on the configuration of the snakeboard coupler in $SE(2)$, we define $\xi = (x, y, \theta) \in SE(2)$ to be the projection of the full configuration q down to the coupler configuration space. From the origin $\xi_0 = (0, 0, 0)$, a two-dimensional set $\Xi_R \subset SE(2)$ is reachable by a single \mathcal{R} motion (i.e., a sequence \mathcal{WR}):

$$\begin{aligned} \Xi_R &= \{(x_G, y_G, \theta_G) \mid \exists (R, \theta) \in \mathbb{R} \times [0, 2\pi) : \\ &\quad (x_G, y_G, \theta_G) = (R \sin \theta, R(1 - \cos \theta), \theta)\}. \end{aligned}$$

The set Ξ_R can be identified with the set of all circles (of finite radius) tangent to the x -axis at the origin. These circles have centers at $(0, R)$, where R is related to the wheel angle ϕ by

$$R = \ell \cot \phi.$$

²Note that problem RP is similar to path planning for a car unable to drive in a straight line but with no minimum turning radius.

Note that it is possible to set $R = 0$ by steering the wheels to an angle $\phi = \pm\pi/2$, meaning that Ξ_R contains the “spin in place” configurations $(0, 0, \theta)$.

A goal configuration $\xi_G \in \Xi_R$ represents a singular case, as Ξ_R is a two-dimensional submanifold of $SE(2)$. Generically, more than one \mathcal{R} motion is required. Consider any goal position and orientation $\xi_G = (x_G, y_G, \theta_G)$ not of the form $(x_G, 0, 0)$. In this case, it is possible to steer the snakeboard from ξ_0 to ξ_G with two \mathcal{R} motions. One \mathcal{R} motion is used to steer the snakeboard from ξ_0 to a *switch point* and another \mathcal{R} motion is used to steer the snakeboard from the switch point to the goal. For a given ξ_G , there exists a set of possible switch points on the plane defining a *switch curve* \mathcal{S} . This switch curve is defined by points on the plane where two sets of circles are tangent to each other: the set of all circles tangent to the x -axis at $x_0 = 0$, and the set of all the circles tangent to a line at (x_G, y_G) at angle θ_G . In general, a switch curve will be a circle itself.

The switch curve can be found geometrically as follows for the case $\theta_G \neq 0, \pi$. Define the points $O = (0, 0)$ and $G = (x_G, y_G)$ corresponding to the initial and goal positions, respectively. The common center of rotation C for the initial and goal configurations can be found by intersecting the lines through O and G perpendicular to the heading directions (Fig. 2). Point C has coordinates $(x_C, y_C) = (0, y_G + x_G \cot \theta_G)$. Also define points $A = (0, y_C + \|C - G\|)$ and $B = (0, y_C - \|C - G\|)$. The circle \mathcal{A} , defined by the points O, G, A , and the circle \mathcal{B} , defined by the points O, G, B , are switch curves. If $x_G / \sin \theta_G > 0$, circle \mathcal{A} is the relevant switch curve, and if $x_G / \sin \theta_G < 0$, circle \mathcal{B} is the relevant switch curve. The other switch curve results in a final orientation $\theta_G + \pi$. In the case that $x_G = 0$, the switch circles may be constructed in the same way, exchanging the roles of the initial and goal configurations.

Any point on a switch curve can be chosen as a switch point, except those on a line through O along the initial heading direction (the x -axis), or those on a line through G along the final heading direction. We call these “blind spots.” These points are not valid switch points, as the snakeboard cannot translate under the rotor action. Figure 3 shows switch circles, blind spots, and example paths for $\xi_G = (1, 2, \pi/3)$.

A degenerate case occurs when $\theta_G = 0$ or π . The switch curve for $\theta_G = 0$ becomes an infinite radius circle, specifically a switch *line* through O and G . For $\theta_G = \pi$, the switch curve is the circle through O and G with diameter $\|O - G\|$. In both cases, two \mathcal{R} motions are required to go from O to G .

Only for goal configurations $\xi_G = (x_G \neq 0, 0, 0)$ is there no sequence of two \mathcal{R} motions accomplishing the task. This is because the switch curve, the line through O and G , becomes the x -axis, and all points of the switch curve are blind spots for both ξ_0 and ξ_G . Therefore, a preliminary \mathcal{R} motion is needed to move the snakeboard out of this singular configuration, and a total of three \mathcal{R} motions are required to steer the snakeboard from ξ_0 to ξ_G , as shown in Fig. 4. Goal configurations of the form $(x_G \neq 0, 0, 0)$ form a one-dimensional singular submanifold.

Now we take the \mathcal{W} motions into account. When $(x_G, y_G, \theta_G) = (\ell \cot \phi_0 \sin \theta_G, (1 - \cos \theta_G) \ell \cot \phi_0, \theta_G)$, then the initial wheel angle $\phi_0 \neq 0$ allows the goal to be reached with a single \mathcal{R} motion. For all other $\xi_G \in \Xi_R$, the goal can be reached by steering the wheels and then activating the rotor.

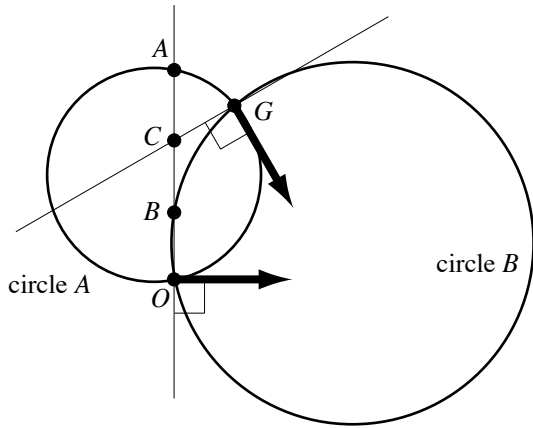


Fig. 2. Geometric construction of the switch curve.

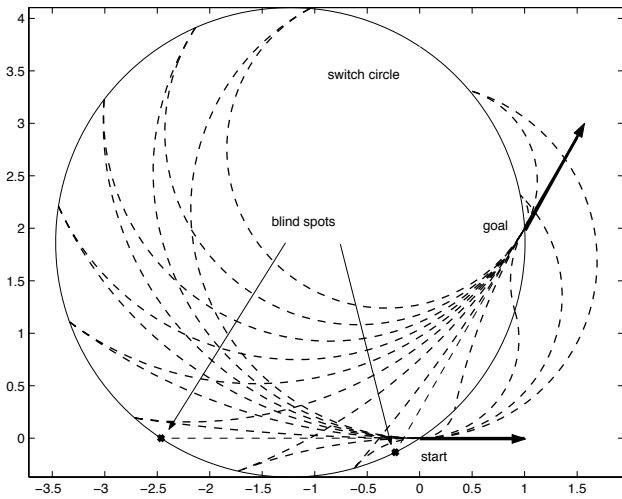


Fig. 3. The switch circle for $\xi_G = (1, 2, \pi/3)$, the blind spots, and example paths.

In the generic case with $\phi_0 \neq 0$, two \mathcal{R} motions are required, and a plan consists of three motions, \mathcal{RWR} . In this case, $\xi_0 = (0, 0, 0)$ and ξ_G define a switch curve, and the initial steering angle ϕ_0 determines a switch point on the switch curve. After performing the first \mathcal{R} motion to reach the switch point, the wheels are steered to take the coupler to the goal configuration by the second \mathcal{R} motion. In the singular case that $\phi_0 = 0$, we must perform an initial \mathcal{W} motion to choose a switch point away from the blind spot. Similarly, if the switch point defined by ξ_0 and ϕ_0 is at a blind spot for ξ_G , defined by the condition

$$((\ell \cot \phi_0 - y_G) \cos \theta_G + x_G \sin \theta_G)^2 = \ell^2 \cot^2 \phi_0,$$

we must perform an initial \mathcal{W} motion to choose a different switch point, feasible for ξ_G .

All the possible cases are summarized in Table I. These results lead to the following proposition.

Proposition 1: Given any initial configuration $q_0 = (0, 0, 0, 0, \phi_0)$ and any goal configuration manifold $\mathcal{Q}_1 = \{q \in \mathcal{Q} | q = (x_G, y_G, \theta_G, \cdot, \cdot)\}$, we have $l_{\min}(q_0, \mathcal{Q}_1) \leq 6$. For generic q_0 and \mathcal{Q}_1 , there exists a plan \mathcal{P} connecting q_0 to \mathcal{Q}_1 such that $l(\mathcal{P}) = 3$.

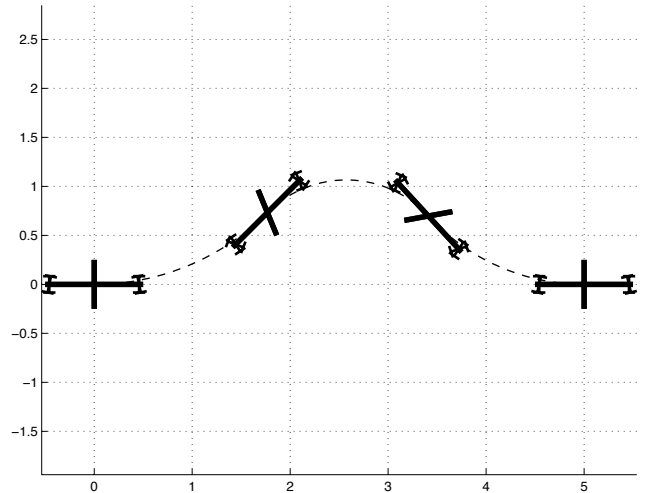


Fig. 4. A singular situation that requires three \mathcal{R} motions.

VI. THE FULL PROBLEM

Problem FP considers all configuration variables q of the snakeboard. We can see immediately that $l_{\min}(q_0, q_G) \leq 9$ for any q_0, q_G . This follows from the fact that the maximum plan length for the reduced problem RP is six. The full problem can be solved by first driving the snakeboard to (x_G, y_G, θ_G) , and then appending the sequence $\mathcal{W}_0 \mathcal{R}_{\psi_G} \mathcal{W}_{\phi_G}$ to account for the desired wheel and rotor angles.

This simple bound is improved by the following proposition.

Proposition 2: Given any initial configuration $q_0 = (0, 0, 0, 0, \phi_0)$ and any goal configuration $q_G = (x_G, y_G, \theta_G, \psi_G, \phi_G)$, we have $l_{\min}(q_0, q_G) \leq 7$. For generic q_0 and q_G , there exists a plan \mathcal{P} connecting q_0 to q_G such that $l(\mathcal{P}) = 5$.

The proof of this proposition is omitted for space. The approach can be understood intuitively as follows. As in the reduced problem RP, most reconfigurations of the snakeboard body can be accomplished with two \mathcal{R} motions, and there is a one-dimensional family of solutions described by the switch curve \mathcal{S} . This one-dimensional family of solutions can be parameterized by the wheel angle ϕ_1 and the body rotation direction $\Omega_1 \in \{\text{CW}, \text{CCW}\}$ during the first \mathcal{R} motion. We can then define the total rotor angular displacement during the motion from q_0 to q_G to be a function of ϕ_1, Ω_1 , that is, $\Delta\psi(\phi_1, \Omega_1)$. It is easy to show that this function is onto \mathbb{R} — any rotor displacement is possible by appropriate choice of ϕ_1, Ω_1 . For a desired ψ_G , we simply perform a numerical search on the function $\Delta\psi$. We can choose bounds on the search within which a solution is guaranteed to exist, and since the function is smooth within these bounds, there are many numerical methods which can be used to solve for ϕ_1 . We used Matlab's `fzero` function.

Therefore, in the generic case, a plan of the form \mathcal{WRWRW} will solve the full problem FP. The first wheel motion \mathcal{W} chooses a switch point on the switch curve so that after the subsequent \mathcal{RWR} motion to the goal body configuration ξ_G , the rotor angle will be at ψ_G . The final \mathcal{W} motion turns the wheels to ϕ_G . The worst case occurs when $q_G = (x_G \neq 0, 0, 0, \cdot, 0)$; this requires a length seven plan of the form $\mathcal{WRWRWRW}$, where the first six motions are identical to those in the RP case.

x_G, y_G, θ_G	ϕ_0	l_{\min}	Plan
Generic case	$\phi_0 \neq 0$	3	$\mathcal{R}_{\Delta\psi_1} \mathcal{W}_{\phi_1} \mathcal{R}_{\Delta\psi_2}$
	$\phi_0 = 0$ or $((\ell \cot \phi_0 - y_G) \cos \theta_G + x_G \sin \theta_G)^2 = \ell^2 \cot^2 \phi_0$	4	$\mathcal{W}_{\phi_1} \mathcal{R}_{\Delta\psi_1} \mathcal{W}_{\phi_2} \mathcal{R}_{\Delta\psi_2}$
$(x_G, y_G, \theta_G) = (R \sin \theta, R(1 - \cos \theta), \theta)$	$\phi_0 \neq 0, R = \ell \cot \phi_0$	1	$\mathcal{R}_{\Delta\psi_1}$
	else	2	$\mathcal{W}_{\phi_1} \mathcal{R}_{\Delta\psi_1}$
$x_G \neq 0, y_G = \theta_G = 0$	$\phi_0 = 0$	6	$\mathcal{W}_{\phi_1} \mathcal{R}_{\Delta\psi_1} \mathcal{W}_{\phi_2} \mathcal{R}_{\Delta\psi_2} \mathcal{W}_{\phi_3} \mathcal{R}_{\Delta\psi_3}$
	$\phi_0 \neq 0$	5	$\mathcal{R}_{\Delta\psi_1} \mathcal{W}_{\phi_1} \mathcal{R}_{\Delta\psi_2} \mathcal{W}_{\phi_2} \mathcal{R}_{\Delta\psi_3}$
$x_G = y_G = \theta_G = 0$	any	0	—

TABLE I
LIST OF MINIMUM CONTROL SWITCH PLANS FOR PROBLEM RP.

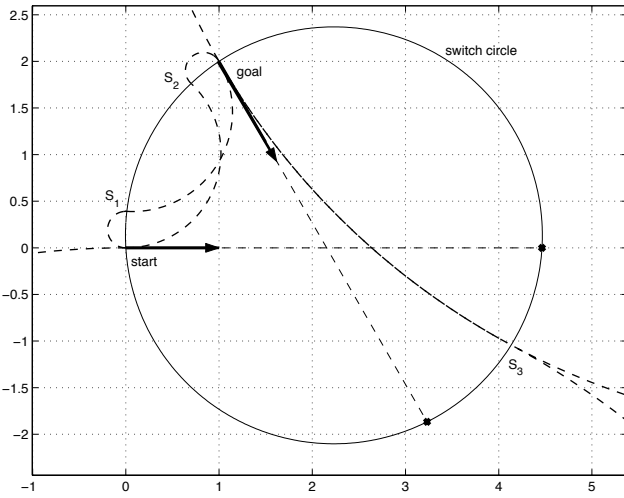


Fig. 5. The three computed paths. One of the paths goes far outside the figure.

We have written Matlab code to calculate minimum control switch motion plans for the snakeboard. As a complete example, choose $q_G = (1, 2, -\pi/3, 0, 0)$ and the following parameters for the snakeboard: $\ell = 0.5, m = J = J_r = 1, J_w = 0.25$. Our numerical search for solutions to $\Delta\psi(\phi_1, \Omega_1) = 0$ yields three solutions, as shown in Figure 5. (There are other solutions with the same number of control switches, but none with less.) Of the three plans, the one minimizing total rotor motion and path length is shown in Figure 6. The complete plan is $\mathcal{P} = \mathcal{W}_{\phi_1} \mathcal{R}_{\Delta\psi_1} \mathcal{W}_{\phi_2} \mathcal{R}_{\Delta\psi_2} \mathcal{W}_{\phi_3}$, with $\phi_1 = 1.1978$ rad, $\phi_2 = -0.4358$ rad, $\Delta\psi_1 = -\Delta\psi_2 = 7.3152$ rad.

Table II gives an exhaustive list of optimal motions for the snakeboard as a function of the initial and goal configurations.

VII. CONCLUSIONS AND FUTURE WORK

We have implemented code in Matlab to calculate the minimum segment paths described in this paper. Our next step is to incorporate this code into a collision-free motion planner for an experimental snakeboard recently constructed in our lab. This snakeboard is similar to the snakeboard of Ostrowski *et al.* [15], [19], except we have equipped it with “training wheels” to allow it the full steering range $\phi \in [-\pi/2, \pi/2]$ without falling over. Experimental results will be reported in a future paper.

One possibility for motion planning for the snakeboard is to

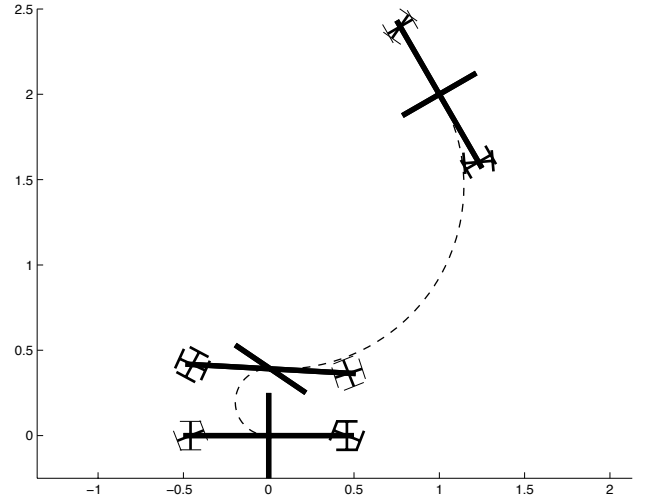


Fig. 6. The computed plan corresponding to selection of switch point S_1 . (In this figure, the rotor angle is shown offset by $\pi/2$ for clarity.)

use a probabilistic roadmap (PRM) motion planner. This approach consists of sampling points in the configuration space, determining if they are collision-free, and if so, attempting to use a simple local planner to connect them to a “roadmap” representation of the free space. The motion planner described in this paper runs quickly and can be used as the local planner, much as Reeds-Shepp curves can be used for motions of cars. Alternatively, we could modify the approach of Laumond *et al.* [9] for motion planning for car-like robots, which uses a holonomic motion planner in a first phase and then recursively replaces segments of the path with motions satisfying the nonholonomic constraint. Initial work in this direction is reported in [7].

Our philosophy for trajectory planning for underactuated mechanical systems is to use the structure of the system equations to reduce the computational complexity when possible. We can take advantage of the kinematic controllability properties of the snakeboard system to decouple trajectory planning into kinematic path planning followed by time-scaling to execute the trajectory quickly. Since the system must come to rest when switching between decoupling vector fields, it is important to minimize the number of switches in the path planning phase. This paper has derived the minimum-switch motion plans for a snakeboard in an obstacle-free environment.

x_G, y_G, θ_G	ϕ_0, ϕ_G, ψ_G	l_{\min}	Plan
Generic case	$\phi_0 \neq \phi_1, \phi_G \neq \phi_2, \Delta\psi_1 + \Delta\psi_2 = \psi_G$	5	$\mathcal{W}_{\phi_1} \mathcal{R}_{\Delta\psi_1} \mathcal{W}_{\phi_2} \mathcal{R}_{\Delta\psi_2} \mathcal{W}_{\phi_G}$
	$\phi_0 \neq \phi_1, \phi_G = \phi_2, \Delta\psi_1 + \Delta\psi_2 = \psi_G$	4	$\mathcal{W}_{\phi_1} \mathcal{R}_{\Delta\psi_1} \mathcal{W}_{\phi_2} \mathcal{R}_{\Delta\psi_2}$
	$\phi_0 = \phi_1, \phi_G \neq \phi_2, \Delta\psi_1 + \Delta\psi_2 = \psi_G$	4	$\mathcal{R}_{\Delta\psi_1} \mathcal{W}_{\phi_2} \mathcal{R}_{\Delta\psi_2} \mathcal{W}_{\phi_G}$
	$\phi_0 = \phi_1, \phi_G = \phi_2, \Delta\psi_1 + \Delta\psi_2 = \psi_G$	3	$\mathcal{R}_{\Delta\psi_1} \mathcal{W}_{\phi_2} \mathcal{R}_{\Delta\psi_2}$
$(x_G, y_G, \theta_G) = (R \sin \theta, R(1 - \cos \theta), \theta)$	$\phi_0 = 0, \phi_1 = \phi_G, \Delta\psi_1 = \psi_G$	2	$\mathcal{W}_{\phi_1} \mathcal{R}_{\Delta\psi_1}$
	$\phi_0 = 0, \phi_1 \neq \phi_G, \Delta\psi_1 = \psi_G$	3	$\mathcal{W}_{\phi_1} \mathcal{R}_{\Delta\psi_1} \mathcal{W}_{\phi_G}$
	$\phi_0 = \phi_G \neq 0, R = l \cot \phi_0, \Delta\psi_1 = \psi_G$	1	$\mathcal{R}_{\Delta\psi_1}$
	$\phi_0 = \phi_G \neq 0, R = l \cot \phi_0, \Delta\psi_1 \neq \psi_G$	4	$\mathcal{R}_{\Delta\psi_1} \mathcal{W}_0 \mathcal{R}_{\psi_G} \mathcal{W}_{\phi_G}$
	$\phi_0 \neq \{0, \phi_G\}, R = l \cot \phi_0, \Delta\psi_1 = \psi_G$	2	$\mathcal{R}_{\Delta\psi_1} \mathcal{W}_{\phi_G}$
	$\phi_0 \neq \{0, \phi_G\}, R = l \cot \phi_0, \Delta\psi_1 \neq \psi_G$	4	$\mathcal{R}_{\Delta\psi_1} \mathcal{W}_0 \mathcal{R}_{\psi_G} \mathcal{W}_{\phi_G}$
	$\phi_0 \neq 0, R \neq l \cot \phi_0, R = l \cot \phi_G, \Delta\psi_1 = \psi_G$	2	$\mathcal{W}_{\phi_G} \mathcal{R}_{\Delta\psi_1}$
	$\phi_0 \neq 0, R \neq l \cot \phi_0, \phi_G = 0, \Delta\psi_1 \neq \psi_G$	4	$\mathcal{W}_{\phi_1} \mathcal{R}_{\Delta\psi_1} \mathcal{W}_{\phi_G} \mathcal{R}_{\psi_G}$
	$\phi_0 \neq 0, R \neq l \cot \phi_0, \phi_1 \neq \phi_G, \Delta\psi_1 = \psi_G$	3	$\mathcal{W}_{\phi_1} \mathcal{R}_{\Delta\psi_1} \mathcal{W}_{\phi_G}$
else	5	$\mathcal{W}_{\phi_1} \mathcal{R}_{\Delta\psi_1} \mathcal{W}_0 \mathcal{R}_{\psi_G} \mathcal{W}_{\phi_G}$	
$x_G \neq 0, y_G = \theta_G = 0$	$\phi_0 = 0, \phi_3 = \phi_G \neq 0, \Delta\psi_1 + \Delta\psi_2 + \Delta\psi_3 = \psi_G$	6	$\mathcal{W}_{\phi_1} \mathcal{R}_{\Delta\psi_1} \mathcal{W}_{\phi_2} \mathcal{R}_{\Delta\psi_2} \mathcal{W}_{\phi_G} \mathcal{R}_{\Delta\psi_3}$
	$\phi_0 = \phi_G = 0$	7	$\mathcal{W}_{\phi_1} \mathcal{R}_{\Delta\psi_1} \mathcal{W}_{\phi_2} \mathcal{R}_{\Delta\psi_2} \mathcal{W}_{\phi_3} \mathcal{R}_{\Delta\psi_3} \mathcal{W}_{\phi_G}$
	$\phi_0 \neq 0, \phi_3 = \phi_G \neq 0, \Delta\psi_1 + \Delta\psi_2 + \Delta\psi_3 = \psi_G$	5	$\mathcal{R}_{\Delta\psi_1} \mathcal{W}_{\phi_2} \mathcal{R}_{\Delta\psi_2} \mathcal{W}_{\phi_3} \mathcal{R}_{\Delta\psi_3}$
	$\phi_0 \neq 0, \phi_G = 0$	6	$\mathcal{R}_{\Delta\psi_1} \mathcal{W}_{\phi_2} \mathcal{R}_{\Delta\psi_2} \mathcal{W}_{\phi_3} \mathcal{R}_{\Delta\psi_3} \mathcal{W}_{\phi_G}$
$x_G = y_G = \theta_G = 0$	$\phi_0 = \phi_G, \psi_0 = \psi_G$	0	—
	$\phi_0 = \phi_G = 0, \psi_0 \neq \psi_G$	1	\mathcal{R}_{ψ_G}
	$\phi_G \neq \phi_0, \psi_0 = \psi_G$	1	\mathcal{W}_{ϕ_G}
	else	3	$\mathcal{W}_0 \mathcal{R}_{\psi_G} \mathcal{W}_{\phi_G}$

TABLE II
LIST OF MINIMUM CONTROL SWITCH PLANS FOR PROBLEM FP.

ACKNOWLEDGMENTS

The work of the first author was supported in part by the Antonio Ruberti grant funded by the Università di Roma “La Sapienza.” The work of the second author is supported by NSF grant IIS-9811571. Thanks to Eric Faulring, Marin Zimbru, Stanley Tsao, and Ben Stephens for building the snakeboard.

REFERENCES

- [1] D. J. Balkcom and M. T. Mason, “Time optimal trajectories for differential drive vehicles,” *International Journal of Robotics Research*, vol. 21, no. 3, pp. 199–217, March 2002.
- [2] J. E. Bobrow, S. Dubowsky, and J. S. Gibson, “Time-optimal control of robotic manipulators along specified paths,” *International Journal of Robotics Research*, vol. 4, no. 3, pp. 3–17, 1985.
- [3] F. Bullo and A. D. Lewis, “Kinematic controllability and motion planning for the snakeboard,” to appear in *IEEE Trans. on Robotics and Automation*, 2003.
- [4] F. Bullo, A. D. Lewis, and K. M. Lynch, “Controllable kinematic reductions for mechanical systems: Concepts, computational tools, and examples,” *2002 Int. Symp. on Mathematical Theory of Networks and Systems (MTNS 2002)*, Notre Dame, IL, USA, 2002.
- [5] F. Bullo and K. M. Lynch, “Kinematic controllability for decoupled trajectory planning in underactuated mechanical systems,” *IEEE Trans. on Robotics and Automation*, vol. 17, no. 4, pp. 402–412, 2001.
- [6] F. Bullo and M. Zefran, “On mechanical control systems with nonholonomic constraints and symmetries,” *Systems and Control Letters*, vol. 45, no. 2, pp. 133–143, Jan. 2002.
- [7] P. Choudhury and K. M. Lynch, “Trajectory planning for kinematically controllable underactuated mechanical systems,” *Fifth Workshop on the Algorithmic Foundations of Robotics*, Nice, France, December 2002.
- [8] L. E. Dubins, “On curves of minimal length with a constraint on average curvature and with prescribed initial and terminal positions and tangents,” *American J. of Mathematics*, vol. 79, pp. 497–516, 1957.
- [9] J.-P. Laumond and P. E. Jacobs and M. Taïx and R. M. Murray, “A motion planner for nonholonomic mobile robots,” *IEEE Transactions on Robotics and Automation*, vol. 10, no. 5, pp. 577–593, October 1994.
- [10] A. D. Lewis, “When is a mechanical control system kinematic?,” *IEEE 38th Conf. on Decision and Control*, Phoenix, AZ, pp. 1162–1167, 1999.
- [11] A. D. Lewis, “Simple mechanical control systems with constraints,” *IEEE Trans. on Automatic Control*, vol. 45, no. 8, pp. 1420–1436, 2000.
- [12] G. Liu and Z. Li, “A unified geometric approach to modeling and control of constrained mechanical systems,” *IEEE Transactions on Robotics and Automation*, vol. 18, no. 4, pp. 574–587, August 2002.
- [13] K. M. Lynch, N. Shiroma, H. Arai, and K. Tanie, “Collision free trajectory planning for a 3-DOF robot with a passive joint,” *Int. J. of Robotics Research*, vol. 19, no. 12, pp. 1171–1184, 2000.
- [14] R. M. Murray and S. S. Sastry, “Nonholonomic motion planning: Steering using sinusoids,” *Trans. on Automatic Control*, vol. 38, n. 5, pp. 700–716, 1993.
- [15] J. Ostrowski, A. Lewis, R. Murray, and J. Burdick, “Nonholonomic mechanics and locomotion: the Snakeboard example,” *IEEE Intl. Conf. on Robotics and Automation*, San Diego, pp. 2391–2400, 1994.
- [16] J. Ostrowski and J. Burdick, “Controllability tests for mechanical systems with constraints and symmetries,” *J. of Applied Mathematics and Computer Science*, vol. 7, no. 2, pp. 101–127, 1997.
- [17] J. Ostrowski and J. Burdick, “The geometric mechanics of undulatory robotic locomotion,” *Int. J. of Robotics Research*, vol. 17, no. 7, pp. 683–701, 1998.
- [18] J. Ostrowski, “Steering for a class of dynamic nonholonomic systems,” *IEEE Trans. on Automatic Control*, vol. 45, no. 8, pp. 1492–1497, 2000.
- [19] J. Ostrowski, J.P. Desai, and V. Kumar, “Optimal gait selection for nonholonomic locomotion systems,” *Int. J. of Robotics Research*, vol. 19, no. 3, pp. 225–237, 2000.
- [20] J. A. Reeds and R. A. Shepp, “Optimal paths for a car that goes both forwards and backwards,” *Pacific J. of Mathematics*, vol. 145, no. 2, 1990.
- [21] K. G. Shin and N. D. McKay, “Minimum-time control of robotic manipulators with geometric path constraints,” *IEEE Transactions on Automatic Control*, vol. 30, no. 6, pp. 531–541, 1985.
- [22] P. Souères and J. P. Laumond, “Shortest path synthesis for a car-like robot,” *IEEE Trans. on Automatic Control*, vol. 41, no. 5, pp. 672–688, 1996.
- [23] H. J. Sussmann and W. Tang, “Shortest paths for the Reeds-Shepp car: a worked out example of the use of geometric techniques in nonlinear optimal control,” *Report SYCON-91-10*, Rutgers University, 1991.